JACS
JOURNAL OF THE AMERICAN CHEMICAL SOCIETY

Communication

pubs.acs.org/JACS

Modulation of Y_{356} Photooxidation in *E. coli* Class Ia Ribonucleotide Reductase by Y_{731} Across the α_2:β_2 Interface

Arturo A. Pizano,[†,‡] Lisa Olshansky,[†,‡] Patrick G. Holder,[†,‡] JoAnne Stubbe,*[,†] and Daniel G. Nocera*[,‡]

[†]Department of Chemistry, Massachusetts Institute of Technology, 77 Massachusetts Avenue, Cambridge, Massachusetts 02139, United States

[‡]Department of Chemistry and Chemical Biology, 12 Oxford Street, Harvard University, Cambridge, Massachusetts 02138, United States

Supporting Information

ABSTRACT: Substrate turnover in class Ia ribonucleotide reductase (RNR) requires reversible radical transport across two subunits over 35 Å, which occurs by a multistep proton-coupled electron-transfer mechanism. Using a photooxidant-labeled β_2 subunit of *Escherichia coli* class Ia RNR, we demonstrate photoinitiated oxidation of a tyrosine in an α_2:β_2 complex, which results in substrate turnover. Using site-directed mutations of the redox-active tyrosines at the subunit interface, $Y_{356}F(\beta)$ and $Y_{731}F(\alpha)$, this oxidation is identified to be localized on Y_{356}. The rate of Y_{356} oxidation depends on the presence of Y_{731} across the interface. This observation supports the proposal that unidirectional PCET across the $Y_{356}(\beta)$−$Y_{731}(\alpha)$−$Y_{730}(\alpha)$ triad is crucial to radical transport in RNR.

Ribonucleotide reductases (RNRs) catalyze the conversion of nucleoside diphosphates (NDPs) to deoxynucleoside diphosphates (dNDPs) in all organisms. As such, they are largely responsible for maintaining the balanced cellular pools of DNA precursors.[1] While NDP reduction occurs by a highly conserved radical-based mechanism in the class I and II RNRs, the class Ia enzyme represents a unique and remarkable example of radical transport in biology.

Class Ia RNR consists of two homodimeric subunits, α_2 and β_2. Turnover requires reversible radical transport from the resting location of the radical, $Y_{122}(\beta)$, to the active site, $C_{439}(\alpha)$. These sites are separated by 35 Å, as predicted by a docking model[2] of both subunits and recently confirmed by pulsed electron−electron double resonance (PELDOR)[3] and small-angle X-ray scattering.[4] Any single-step radical transport mechanism over this distance is incongruent with the observed rate of turnover (2−10 s^{-1}). Consequently, multistep radical transfer through a pathway involving a number of highly conserved redox-active aromatic amino acids has been proposed, $Y_{122}\rightarrow[W_{48}?]\rightarrow Y_{356}$ in β_2 to $Y_{731}\rightarrow Y_{730}\rightarrow C_{439}$ in α_2, Figure 1.[7,8] Amino acid radical generation requires removal of both a proton and an electron. One-electron oxidized or deprotonated intermediates are thermodynamically inaccessible under physiological conditions, implicating a proton-coupled electron transfer (PCET) mechanism for radical initiation and transport.

In an effort to probe the mechanism of the long-range radical transport, we developed a series of photochemical RNR constructs.[9] In these constructs, the β_2 subunit is replaced by a short peptide encompassing the 20 *C*-terminal residues of the β_2 protein, which includes the binding determinant for α_2 as well as a conserved tyrosine residue in a position analogous to Y_{356}.[10] By appending a photooxidant to the *N*-terminus of this peptide, tyrosyl radicals can be photochemically generated, thereby enabling detailed studies of photoinitiated substrate turnover,[11] spectroscopic observation of photogenerated radicals,[12] and direct measurement of radical injection rates into α_2.[13] In using these peptide constructs, we found that the weak association between the peptide and the α_2 subunit ($K_D \sim 10\ \mu M$) and the conformational flexibility of the bound peptide[14] inhibit radical injection and complicate the examination of PCET kinetics.

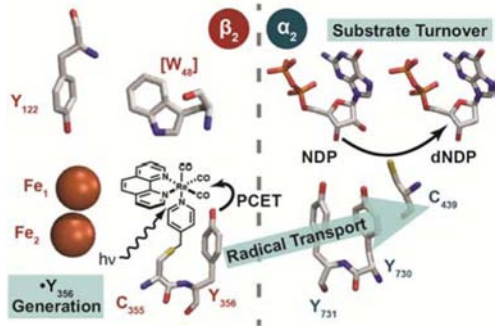

Figure 1. An intact, photochemical RNR where a radical is generated directly at $Y_{356}(\beta)$ and is poised to follow the proposed radical transport pathway through α_2 to the active site. Figure prepared from PDB codes 4R1R[5] (α_2) and 1MXR[6] (β_2).

To address these challenges and to develop a faithful construct of the natural system, we recently developed a full-length photochemical β_2 subunit.[15] In this construct, a bromomethylpyridyl rhenium(I) tricarbonyl phenanthroline complex selectively modifies a single surface-accessible cysteine variant at position 355 of *E. coli* class Ia β_2 to yield a labeled subunit ([Re]−β_2). Upon excitation of the [Re] complex, a transient tyrosyl radical forms and can be spectroscopically detected.[15] We now report the photochemical generation of $\bullet Y_{356}$ in an intact α_2:β_2 complex, which is competent for photoinitiated substrate turnover. To decipher the nature of tyrosine oxidation processes by [Re] at the subunit interface, the $Y_{356}F$ variant ([Re]−$Y_{356}F$−β_2) was prepared. By performing a comparative transient

Received: June 1, 2013
Published: August 8, 2013

   dx.doi.org/10.1021/ja405498e | *J. Am. Chem. Soc.* 2013, 135, 13250−13253

kinetics study of α_2:[Re]−Y_{356}F−β_2 and [Re]−β_2:Y_{731}F−α_2 constructs, a photooxidation process to furnish radicals is ascribed to interfacial tyrosine radical transport.

The [Re] group does not preclude binding of [Re]−β_2 to α_2. A competitive inhibition assay (Figure S1)[10] reveals that the observed dissociation constant (K_D([Re]−β_2) = 0.71(8) μM) is comparable to that observed for aminotyrosine (NH_2Y) substituted β_2.[16] With binding established, RNR activity assays were performed on the unlabeled S_{355}C−β_2 and labeled [Re]−β_2 to ascertain the effect of labeling on activity. The 1100 U/mg (Figure S2) activity of unlabeled S_{355}C−β_2 is less than β_2 (7600 U/mg)[17] and decreases further upon labeling to 122 U/mg. The low observed activity of [Re]−β_2, despite only a modest reduction in subunit binding affinity, suggests a subtle as opposed to a large perturbation to the protein structure. To avoid complications from steady-state activity, [Re]−β_2 was treated with hydroxyurea (HU) to reduce the native radical cofactor ($\bullet Y_{122}$), yielding met−[Re]−β_2. This form was used for all experiments except the above activity assays and is subsequently referred to as [Re]−β_2 for convenience.

The efficacy of photooxidant labeling is revealed by activity measurements of [Re]−β_2 under illumination (λ > 325 nm) and in the presence prereduced wt−α_2, where wt−α_2 are reduced, but there is no additional reductant available. Figure 2 shows that

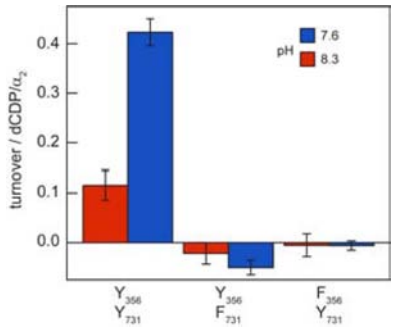

Figure 2. Photochemical substrate turnover in the α_2:[Re]−β_2 complex formed from met−[Re]−β_2 or met−[Re]−Y_{356}F−β_2 and prereduced wt−α_2 or Y_{731}F−α_2 (as indicated) at pH 8.3 (50 μM [Re]−β_2, 20 μM α_2, 50 mM borate, 15 mM $MgSO_4$, 1 mM EDTA, 0.2 mM [^{3}H]-CDP (10 750 cpm/nmol), 3 mM ATP, 5% glycerol) or pH 7.6 (30 μM [Re]−β_2, 10 μM α_2, 50 mM HEPES, 15 mM $MgSO_4$, 0.2 mM [^{3}H]-CDP (22 713 cpm/nmol), 3 mM ATP), λ_e > 325 nm.

dCDP product is formed at 0.47(3) dCDP/α_2 (pH 7.6) or 0.11(2) dCDP/α_2 (pH 8.3) under photochemical conditions. The identity of the product was confirmed by an HPLC assay (Figure S3). This product yield is less than that observed previously for photoRNRs consisting of a peptide surrogate for β_2 in the presence of wt−α_2 (~0.2 dCDP/α_2).[12] However, we note that in the peptide surrogate, position 356 on the peptide was occupied by 3,5-difluorotyrosine (3,5-F_2Y), as opposed to tyrosine. Greater radical production yield at pH 8.3 is expected for 3,5-F_2Y because the amino acid is deprotonated, and tyrosine is not. Hence, 3,5-F_2Y is more rapidly oxidized than tyrosine, despite having similar reduction potentials at this pH. Consistent with previous peptide-based systems,[12] the phototurnover yield of the α_2:[Re]−β_2 construct is significantly greater and time-dependent at pH 7.6 (Figure S4).

Having established that [Re]−β_2 is photochemically active for substrate turnover, we sought to generate a radical within the α_2:[Re]−β_2 complex. Photoexcitation (λ = 355 nm) of [Re]−β_2 or [Re]−Y_{356}F−β_2 yields transient absorption features (Figure S5) consistent with the ^{3}MLCT excited state ([Re^I]*),[15] but no signatures corresponding to tyrosyl radical are observed. Scheme 1 shows a photophysical model for the system. In the absence of

Scheme 1. Excited-State Deactivation Pathways for [Re^I]*

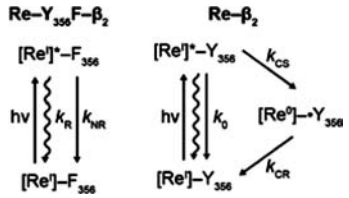

tyrosine (left), the observed lifetime, τ_o is defined by nonradiative (k_{NR}) and radiative (k_R) decay rate constants as follows:

$$1/\tau_o = k_R + k_{NR} \quad (1)$$

For the kinetics associated with the β_2 subunit, τ_o is given by [Re]−Y_{356}F−β_2. For rate constant calculations, measurement of τ_o differs from measurement of the observed lifetime owing to the presence of Y_{356}, as indicated in Table 1. The presence of Y_{356}

Table 1. Tyrosine-Dependent Excited-State Quenching at the α_2:β_2 Interface (pH = 7.6)

β_{356}	α_{731}[a]	τ/ns[b]	$k_{CS}/10^5$ s^{-1}[c]
Y	–	403(31) (= τ_{obs})	8.37(66)
F	–	607(7) (= τ_o)	
Y	Y	543(13) (= τ_{obs})	4.05(10)
F	Y	696(5) (= τ_o)	
Y	F	590(17) (= τ_{obs})	3.28(11)
F	F	732(11) (= τ_o)	

[a]Emission lifetimes measured on samples of 10 μM met−[Re]−β_2 or met−[Re]−Y_{356}F−β_2 and 25 μM wt−α_2 or Y_{731}F−α_2 (as indicated) in 50 mM HEPES, 15 mM $MgSO_4$, 1 mM EDTA, 1 mM CDP, 3 mM ATP, pH 7.6, λ_{exc} = 355 nm, λ_{det} = 600 nm. Representative decay traces are shown in Figure S6. [b]Errors shown in parentheses represent 2σ from triplicate measurements on independently prepared samples. [c]k_{CS} is determined from eq 2. Errors shown in parentheses represent 2σ propagated error of corresponding lifetimes.

in β_2 adds an additional decay pathway via charge separation (k_{CS}), which may be determined from the observed lifetime (τ_{obs}):

$$k_{CS} = 1/\tau_{obs} - 1/\tau_o \quad (2)$$

where τ_{obs} is inversely related to the observed rate constant (k_{obs}) (i.e., $k_{obs} = 1/\tau_{obs}$). The lifetime of [Re^I]* in [Re]−β_2 is significantly shorter than that for the construct with Y_{356} replaced by F, Table 1. We ascribe the shortened lifetime of [Re^I]* in [Re]−β_2 to quenching of [Re^I]* by Y_{356} (Scheme 1). These data suggest that the inability to detect tyrosine radical signal is due to rapid charge recombination of the [Re^0]−•Y charge-separated state ($k_{CR} > k_{CS}$). Using the lifetime of [Re^I]* in [Re]−Y_{356}F−β_2 to provide τ_o, the rate constant for charge separation, k_{CS}, is calculated from eq 2 to be k_{CS} = 8.37(66) × 10^5 s^{-1}. Previously reported charge recombination rate constants for rhenium polypyridine tyrosine systems exceed 10^7 s^{-1}.[18] Accordingly, k_{CR} appears to be much greater than k_{CS}, thus accounting for our inability to observe tyrosyl radical in the transient absorption spectrum.

In the presence of wt−α_2, the lifetime of [Re^I]* is also quenched within the intact α_2:[Re]−β_2 complex. Under these

dx.doi.org/10.1021/ja405498e | J. Am. Chem. Soc. 2013, 135, 13250−13253

conditions, 96% of [Re]−β_2 is bound to α_2. In this α_2:[Re]−β_2 complex, the lifetime of [Re^I]* increases for both [Re]−β_2 and [Re]−Y_{356}F−β_2 (Table 1, Figure S6) because the [Re] center resides in the hydrophobic environment of the protein.[14] Notwithstanding, the lifetime of α_2:[Re]−β_2 is shorter than that of the [Re]−Y_{356}F−β_2 complex, and a charge separation rate constant—again assigned to Y_{356} oxidation—is calculated to be $k_{CS} = 4.05(10) \times 10^5\ s^{-1}$.

The charge separation reaction is affected by perturbations of the radical transport pathway in α_2. When $Y_{731}(\alpha)$ is replaced by phenylalanine, the rate constant for Y_{356} oxidation decreases to $3.28(11) \times 10^5\ s^{-1}$. This difference corresponds to a 23% enchancement in $Y_{356}(\beta)$ oxidation when $Y_{731}(\alpha)$ is present. At pH 8.3, a similar phenomenon is observed (Table S1, Figure S7), with faster charge separation and a rate enhancement due to presence of $Y_{731}(\alpha)$ of 14%. Studies of this process at pH 8.3 were performed to maximize tyrosine oxidation at higher pH; studies at pH 7.6 correspond to the regime where greater phototurnover is observed.

This decrease in the rate of Y_{356} oxidation in the presence of F_{731} provides evidence for direct interaction between $Y_{356}(\beta)$ and $Y_{731}(\alpha)$ in the assembled interface. This result is consistent with our previous work showing that oxidation of α_2 by a photogenerated 2,3,6-trifluorotyrosine radical requires both Y_{731} and Y_{730}.[13] This observation led to the proposal that the $Y_{731}(\alpha)$−$Y_{730}(\alpha)$ dyad is an important element for radical transport. The current observation that Y_{356} photooxidation is modulated by Y_{731} suggests a significant interaction between Y_{356} and Y_{731}, across the α_2:β_2 interface. The present work thus suggests further elaboration to our previous model of a coupled tyrosine dyad to a triad, $Y_{356}(\beta)$−$Y_{731}(\alpha)$−$Y_{730}(\alpha)$, which is responsible for mediating intersubunit radical transport as well as radical transport through α_2 to $C_{439}(\alpha)$ at the active site. This result is in line with the recent observation that a new radical, generated by using a highly oxidizing •$NO_2Y_{122}(\beta)$, equilibrates over Y_{356}, Y_{730}, and Y_{731}.[19]

Given the mechanistic hypothesis that unidirectional PCET operates in the α_2 subunit,[7] even a slight perturbation of the $Y_{356}(\beta)$−$Y_{731}(\alpha)$−$Y_{730}(\alpha)$ triad is likely to have an effect on radical transport. Several related studies have provided insight into the nature of interactions between adjacent pathway tyrosine residues. Hydrogen-bonding interactions involving the tyrosine phenol groups of these residues are a crucial structural element. Such a hydrogen-bonded network is consistent with our observations that removal of one hydroxyl group disrupts the oxidation of an adjacent residue. In support of this model, rapid mixing studies of wt−β_2 and NH_2Y_{730}−α_2 (in the presence of CDP and ATP) result in generation of •$NH_2Y_{730}(\alpha)$ and concomitant loss of •$Y_{122}(\beta)$.[20] Examination of this trapped •NH_2Y_{730} by electron nuclear double resonance and density functional theory suggests a detailed model for the hydrogen-bonding network in α_2 including •NH_2Y_{730}, C_{439}, Y_{731}, and a key water molecule.[21]

The importance of hydrogen bonding on the PCET oxidation of phenols has been well established in studies of small molecule models[22−29] as well in natural systems.[30] Hydrogen bonding is critical to the reduction of the redox-active tyrosine Y_Z in photosystem II and plays a key role in the different oxidation states of the oxygen-evolving complex.

Conformational changes may also occur upon substitution of nearby amino acids of the tyrosine triad. An effect of this type has been previously revealed by the NH_2Y_{730}−α_2 crystal structure; the observed electron density suggests a second conformation for Y_{731}.[17] In the case of an F to Y mutation, a change in conformation may well result from the loss of a hydrogen bond to the substituted residue. A change in the conformation of a tyrosine residue could significantly alter the distance between residues as well as the local environment of the redox-active phenol group.

With the knowledge that [Re]−β_2 is capable of photochemical Y_{356} oxidation to generate an on-pathway radical, we sought to circumvent the limitation imposed by $k_{CR} > k_{CS}$ by employing the flash-quench methodology.[31] When [Re]−β_2 is in the presence of $Ru^{III}(NH_3)_6Cl_3$, [Re^I]* is rapidly quenched to reveal signals for a tyrosyl radical. As previously observed for the rhenium-bipyridine photopeptide system, increased concentrations of quencher not only result in larger observed signals but also in diminished •Y lifetimes, Figure S8.[13] In the presence of the α_2 subunit, less efficient quenching by Ru^{III} is observed, requiring a concentration of 10 mM to obtain adequate radical signals.

The addition of 10 mM $Ru^{III}(NH_3)_6Cl_3$ quenches [Re^I]*; in the absence of α_2, the [Re]−β_2 lifetime is 65 ns. Addition of wt−α_2 to the solution results in a longer [Re^I]* lifetime (137 ns) owing to the decreased solution exposure of the [Re] complex and an attendant decrease in bimolecular quenching by Ru^{III}. The sensitivity of the [Re^I]* lifetime to α_2 provided a method for determining K_D for [Re]−β_2 under flash quench conditions in lieu of the usual coupled assay, which cannot be performed in the presence of $Ru^{III}(NH_3)_6Cl_3$ (Figure S9). Lifetime analysis of the binding shows that the presence of $Ru^{III}(NH_3)_6Cl_3$ does not significantly perturb binding of [Re]−β_2 (K_D([Re]−β_2) = 0.68(21) μM), (Figure S10).

One potential issue when performing experiments at high concentrations of protein (up to 50 μM [Re]−β_2 and 75 μM α_2) is the formation of assemblies larger than α_2:β_2, as previously observed for the inhibited form of *E. coli* Class Ia RNR (formed in the presence of dATP).[4] Under different conditions, such oligomers may not retain an intact subunit interface, precluding the generation of on-pathway radical or its subsequent transport. With 10 μM of each subunit, even in the absence of dATP, species larger than α_2:β_2 are observed by analytical ultracentrifugation.[4] Nevertheless, PELDOR experiments performed at high concentration (100 μM each of α_2:β_2), including those previously discussed,[19] show on-pathway radicals are generated under these conditions, confirming that radical transport is intact at high concentrations.

In the presence of both wt−α_2 and $Ru^{III}(NH_3)_6Cl_3$, photoexcitation of [Re]−β_2 results in a typical •Y absorption feature at 410 nm (Figure 3). Under these experimental conditions, 97% of [Re]−β_2 in solution is bound to α_2. This observation confirms that [Re] is capable of generating •Y in an assembled α_2:β_2 complex. As in the unquenched experiments above, [Re]−Y_{356}F−β_2 and Y_{731}F−α_2 were employed in combination with [Re]−β_2 and wt−α_2 to determine the identity of the photogenerated radical. The presence of visible signals for •Y in the absence of Y_{356} (Figure 3) indicates that the observed signal is not entirely due to •Y_{356}. In fact, signals due to •Y radical persist even in the case where neither interface tyrosine is present, (Figure S11) suggesting that oxidation of an off-pathway tyrosine is also occurring.

Despite these side-reactions under flash-quench conditions, the relative amplitudes of •Y indicate that a significant fraction of the observed signal is due to •Y_{356}. In all cases where Y_{356} is present, the observed amplitude of •Y is greater than the amplitudes observed in any case where Y_{356} is absent (Figure S12). On the basis of single-wavelength kinetics (Figure S11),

dx.doi.org/10.1021/ja405498e | J. Am. Chem. Soc. 2013, 135, 13250−13253

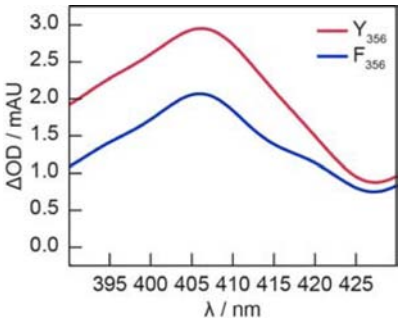

Figure 3. Spectral observation of a photogenerated, Y_{356}-centered tyrosine radical in an α_2:[Re]–β_2 complex. Transient absorption spectra measured 5 μs after excitation on samples of 50 μM met–[Re]–β_2 or met–[Re]–Y_{356}F–β_2 (as indicated), 75 μM wt–α_2, and 10 mM $Ru^{III}(NH_3)_6Cl_3$ in 50 mM borate, 15 mM $MgSO_4$, 1 mM CDP, 3 mM ATP, 5% glycerol, pH 8.3, λ_{exc} = 355 nm.

~44% of the signal is due to $\bullet Y_{356}$. This amplitude corresponds to an estimated quantum yield of 1.2% for overall $\bullet$Y formation and 0.5% for Y_{356}, calculated as previously reported.[15] The presence of the off-pathway radical precludes direct study of radical transport kinetics within the triad.

In this work, we observed rates of tyrosine oxidation in the range of 10^5–10^6 s^{-1}, consistent with PCET oxidation of protonated tyrosine. Future work will target the site-specific installation of a F_nY at $Y_{356}(\beta)$ with established methods[32] in an effort to outcompete off-pathway oxidations by [Re], improve the yield of photogenerated radical, and provide a spectroscopically distinguishable radical signal. The increased acidity of fluorotyrosines allows for their deprotonation, enabling oxidation by electron transfer with rate constants of 10^7–10^9 s^{-1}.[18] Such rapid charge separation enables observation of $\bullet F_nY$ without the necessity of implementing the flash-quench technique. These observed side reactions are expected to play a less significant role in the experiments directly involving $[Re^I]$*, owing to the decreased lifetime and reduction potential of $[Re^I]$* as compared to flash-quench generated $[Re^{II}]$.

Photogeneration of $\bullet Y_{356}$ within an assembled α_2:β_2 complex represents a key advance in the study of PCET in RNRs. The observation of a radical along the α_2 pathway is enabled with the advantages of added fidelity to the natural system and improved subunit binding. This result also opens the door for the study of photoinitiated PCET along the radical transport pathway in the β_2 subunit in the fully assembled protein complex, a longstanding goal of our studies in RNR.

■ ASSOCIATED CONTENT

Ⓢ Supporting Information

Experimental methods and data analysis descriptions. This material is available free of charge via the Internet at http://pubs.acs.org.

■ AUTHOR INFORMATION

Corresponding Author

dnocera@fas.harvard.edu; stubbe@mit.edu

Notes

The authors declare no competing financial interest.

■ ACKNOWLEDGMENTS

We thank Dr. Ellen C. Minnihan and Bryce L. Anderson for helpful discussions. P.G.H. acknowledges the NIH for a postdoctoral fellowship (GM 087034). L.O. acknowledges the NSF for a graduate fellowship. We gratefully acknowledge the NIH for funding (GM 29595 J.S., GM 47274 D.G.N.).

■ REFERENCES

(1) Nordlund, P.; Reichard, P. *Annu. Rev. Biochem.* **2006**, *75*, 681.
(2) Uhlin, U.; Eklund, H. *Nature* **1994**, *370*, 533.
(3) Seyedsayamdost, M. R.; Chan, C. T. Y.; Mugnaini, V.; Stubbe, J.; Bennati, M. *J. Am. Chem. Soc.* **2007**, *129*, 15748.
(4) Ando, N.; Brignole, E. J.; Zimanyi, C. M.; Funk, M. A.; Yokoyama, K.; Asturias, F. J.; Stubbe, J.; Drennan, C. L. *Proc. Natl. Acad. Sci. U.S.A.* **2011**, *108*, 21046.
(5) Eriksson, M.; Uhlin, U.; Ramaswamy, S.; Ekberg, M.; Regnström, K.; Sjöberg, B.-M.; Eklund, H. *Structure* **1997**, *5*, 1077.
(6) Högbom, M.; Galander, M.; Andersson, M.; Kolberg, M.; Hofbauer, W.; Lassmann, G.; Nordlund, P.; Lendzian, F. *Proc. Natl. Acad. Sci. U.S.A.* **2003**, *100*, 3209.
(7) Stubbe, J.; Nocera, D. G.; Yee, C. S.; Chang, M. C. Y. *Chem. Rev.* **2003**, *103*, 2167.
(8) Reece, S. Y.; Nocera, D. G. *Annu. Rev. Biochem.* **2009**, *78*, 673.
(9) Chang, M. C. Y.; Yee, C. S.; Stubbe, J.; Nocera, D. G. *Proc. Natl. Acad. Sci. U.S.A.* **2004**, *101*, 6882.
(10) Climent, I.; Sjöberg, B.-M.; Huang, C. Y. *Biochemistry* **1991**, *30*, 5164.
(11) Reece, S. Y.; Seyedsayamdost, M. R.; Stubbe, J.; Nocera, D. G. *J. Am. Chem. Soc.* **2007**, *129*, 8500.
(12) Reece, S. Y.; Seyedsayamdost, M. R.; Stubbe, J.; Nocera, D. G. *J. Am. Chem. Soc.* **2007**, *129*, 13828.
(13) Holder, P. G.; Pizano, A. A.; Anderson, B. L.; Stubbe, J.; Nocera, D. G. *J. Am. Chem. Soc.* **2012**, *134*, 1172.
(14) Reece, S. Y.; Lutterman, D. A.; Seyedsayamdost, M. R.; Stubbe, J.; Nocera, D. G. *Biochemistry* **2009**, *48*, 5832.
(15) Pizano, A. A.; Lutterman, D. A.; Holder, P. G.; Teets, T. S.; Stubbe, J.; Nocera, D. G. *Proc. Natl. Acad. Sci. U.S.A.* **2012**, *109*, 39.
(16) Minnihan, E. C., Ph.D. Thesis, MIT, 2012.
(17) Minnihan, E. C.; Seyedsayamdost, M. R.; Uhlin, U.; Stubbe, J. *J. Am. Chem. Soc.* **2011**, *133*, 9430.
(18) Reece, S. Y.; Seyedsayamdost, M. R.; Stubbe, J.; Nocera, D. G. *J. Am. Chem. Soc.* **2006**, *128*, 13654.
(19) Yokoyama, K.; Smith, A. A.; Corzilius, B.; Griffin, R. G.; Stubbe, J. *J. Am. Chem. Soc.* **2011**, *133*, 18420.
(20) Seyedsayamdost, M. R.; Xie, J.; Chan, C. T. Y.; Schultz, P. G.; Stubbe, J. *J. Am. Chem. Soc.* **2007**, *129*, 15060.
(21) Argirević, T.; Riplinger, C.; Stubbe, J.; Neese, F.; Bennati, M. *J. Am. Chem. Soc.* **2012**, *134*, 17661.
(22) Sjödin, M.; Irebo, T.; Utas, J. E.; Lind, J.; Merényi, G.; Åkermark, B.; Hammarström, L. *J. Am. Chem. Soc.* **2006**, *128*, 13076.
(23) Johannissen, L. O.; Irebo, T.; Sjödin, M.; Johansson, O.; Hammarström, L. *J. Phys. Chem. B* **2009**, *113*, 16214.
(24) Irebo, T.; Johansson, O.; Hammarström, L. *J. Am. Chem. Soc.* **2008**, *130*, 9194.
(25) Rhile, I. J.; Mayer, J. M. *J. Am. Chem. Soc.* **2004**, *126*, 12718.
(26) Rhile, I. J.; Markle, T. F.; Nagao, H.; DiPasquale, A. G.; Lam, O. P.; Lockwood, M. A.; Rotter, K.; Mayer, J. M. *J. Am. Chem. Soc.* **2006**, *128*, 6075.
(27) Markle, T. F.; Mayer, J. M. *Angew. Chem., Int. Ed.* **2008**, *47*, 738.
(28) Markle, T. F.; Rhile, I. J.; DiPasquale, A. G.; Mayer, J. M. *Proc. Natl. Acad. Sci. U.S.A.* **2008**, *105*, 8185.
(29) Bonin, J.; Costentin, C.; Robert, M.; Savéant, J.-M.; Tard, C. *Acc. Chem. Res.* **2012**, *45*, 372.
(30) Keough, J. M.; Zuniga, A. N.; Jenson, D. L.; Barry, B. A. *J. Phys. Chem. B* **2013**, *117*, 1296.
(31) Chang, I.-J.; Gray, H. B.; Winkler, J. R. *J. Am. Chem. Soc.* **1991**, *113*, 7056.
(32) Minnihan, E. C.; Young, D. D.; Schultz, P. G.; Stubbe, J. *J. Am. Chem. Soc.* **2011**, *133*, 15942.